ADVANCED COMPOSITE SUBSTRATE DEVELOPMENT OF CD-BASED-II-VI MATERIALS FOR IR APPLICATIONS

G. N. Brill, Y. Chen, P. M. Amirtharaj, W. L. Sarney, P. S. Wijewarnasuriya, and N. K. Dhar
U.S. Army Research Laboratory, Sensors and Electron Devices Directorate
AMSRD-ARL-SE-EI, 2800 Powder Mill Rd., Adelphi, MD 20783

ABSTRACT

Through its mature materials development and ability to detect any wavelength of interest within the infrared (IR) spectrum, HgCdTe is currently, and is positioned to remain, the leading choice among IR sensing material for high performance applications. However, a major roadblock lies ahead for HgCdTe IR systems. With array sizes increasing through the need for higher resolution systems, current substrate technology based on bulk CdZnTe material will not be suitable for future systems. The lack of CdZnTe bulk wafer size available (currently limited to less than 7 x 7 cm^2) and high cost in the market place (~\$250/cm^2) will stop the progression of HgCdTe based IR systems.

To mitigate these and other issues, the Army Research Laboratory (ARL) has played a key role in the development of Si-based composite substrate technology for HgCdTe material applications. By transitioning current molecular beam epitaxial (MBE) HgCdTe materials technology to a novel Si-based composite substrate, physical size limitations of HgCdTe material is no longer an issue. Furthermore, besides material cost, manufacturing cost will also be reduced as more dies per wafer will be processed. Specifically, CdTe material technology grown on Si substrates has already been successfully developed for short-wave and mid-wave detector arrays. However, it is recognized that ternary and quarternary Cd-based II-VI materials with lattice matching to that of HgCdTe may be even better suited for HgCdTe growth and IR device processing, particularly for long-wavelength HgCdTe detector arrays. ARL has taken the lead in this research area for the Army.

1. INTRODUCTION

Today, modern war fighters tasked with battlefield management have a critical need to rapidly detect, identify, and constantly survey events in the battlefield. To be effective in this contingency, sensors must continuously view the entire field of regard with ultra high resolution that provides increased probability of detection and identification. It is hoped that the Third Generation Infrared Imaging technology will offer a new suite of products to meet such challenges. The Third Generation family of IR sensors will include very high resolution and high quantum efficiency cooled IR arrays as well as large-format uncooled arrays. It is envisioned that such an enabling technology will facilitate advanced protocols for battlefield management with a suite of sensors that offer high, medium and low performance deployed strategically and activated as needed. Coupled with large-format, multi-color and other sensor products, the Third Generation IR Imaging system will equip the war fighter with the tools needed to maintain dominance in the night.

To achieve ultra high resolution and wide area surveillance capability, very large-format and possibly HDTV (16:9 aspect ratio) format arrays will be necessary. For high performance cooled applications, Mercury Cadmium Telluride ($Hg_{1-x}Cd_xTe$) is the material of choice used for state-of-the-art infrared focal plane array (IRFPA) systems. Through careful control of the alloy composition, the semiconductor can be tuned, within the entire IR spectrum, to detect any wavelength of light, giving a HgCdTe detector array both complex and sensitive detecting abilities. The current material growth process using Molecular Beam Epitaxy (MBE) is to nucleate the HgCdTe layer on a thick, bulk-grown, CdZnTe substrate that is itself lattice-matched to HgCdTe. However, production of very large-format HgCdTe IRFPAs using bulk CdZnTe substrates presents several technology barriers. Bulk CdZnTe substrates are very brittle, costly, relatively small, and have physical limitations when combined with the Si read out integrated circuitry (ROIC) necessary for IRFPA fabrication. These issues make the fabrication of HgCdTe devices extremely costly with a low production yield. Instead of utilizing bulk grown CdZnTe substrates, a thin film of $Cd_{1-y}Zn_yTe$ can be epitaxially deposited directly on a Si substrate using Molecular Beam Epitaxy (MBE). By doing this, the lattice matching property and crystal structure of CdZnTe can be retained. Additionally, the strength, size, and technological maturity of the Si substrate becomes incorporated into the properties of the CdZnTe layer and hence into the HgCdTe material. Therefore using a Si-based substrate template (composite substrate) is very attractive and provides an avenue for a scalable, more reliable, and more affordable alternative towards realizing large-format arrays beyond the limitation posed by the current bulk CdZnTe substrates.

The research effort made during the past few years have already led to a relatively mature MBE growth process for high quality CdTe/Si substrates (Dhar et al,

Report Documentation Page

Form Approved
OMB No. 0704-0188

1. REPORT DATE	2. REPORT TYPE	3. DATES COVERED
00 DEC 2004	**N/A**	**-**

4. TITLE AND SUBTITLE	5a. CONTRACT NUMBER
Advanced Composite Substrate Development Of Cd-Based-Ii-Vi Materials For Ir Applications	5b. GRANT NUMBER
	5c. PROGRAM ELEMENT NUMBER
6. AUTHOR(S)	5d. PROJECT NUMBER
	5e. TASK NUMBER
	5f. WORK UNIT NUMBER
7. PERFORMING ORGANIZATION NAME(S) AND ADDRESS(ES) **U.S. Army Research Laboratory, Sensors and Electron Devices Directorate AMSRD-ARL-SE-EI, 2800 Powder Mill Rd., Adelphi, MD 20783**	8. PERFORMING ORGANIZATION REPORT NUMBER
9. SPONSORING/MONITORING AGENCY NAME(S) AND ADDRESS(ES)	10. SPONSOR/MONITOR'S ACRONYM(S)
	11. SPONSOR/MONITOR'S REPORT NUMBER(S)

12. DISTRIBUTION/AVAILABILITY STATEMENT
Approved for public release, distribution unlimited

13. SUPPLEMENTARY NOTES
See also ADM001736, Proceedings for the Army Science Conference (24th) Held on 29 November - 2 December 2005 in Orlando, Florida. , The original document contains color images.

14. ABSTRACT

15. SUBJECT TERMS

16. SECURITY CLASSIFICATION OF:			17. LIMITATION OF ABSTRACT	18. NUMBER OF PAGES	19a. NAME OF RESPONSIBLE PERSON
a. REPORT	b. ABSTRACT	c. THIS PAGE			
unclassified	**unclassified**	**unclassified**	**UU**	**6**	

1996; Rujirawat et al, 1997). CdTe/Si composite substrates are now the baseline technology and have proven sufficient to grow and fabricate large-format short wavelength (SWIR) and medium wavelength (MWIR) HgCdTe infrared focal plane arrays (Wijewarnarsuriya et al, 1998). Significant progress is still needed to achieve suitable Si-based composite substrates for long-wavelength IRFPAs. Past studies have shown that CdTe/Si technology is not sufficient to achieve optimum quality HgCdTe layers for long-wavelength (8-14 microns) applications due a small, yet significant, lattice mismatch between CdTe and HgCdTe. A scheme to achieve precise lattice matching to HgCdTe with compositions suitable for long-wavelength is necessary. Adding 4% zinc into the CdTe matrix, producing CdZnTe/Si, has been proposed to achieve optimum lattice matching to long-wavelength HgCdTe. Unfortunately, when more than 2% zinc is added in the CdTe matrix, the quality of the CdZnTe layer degrades which negates any advantage that lattice matching might provide. This occurs because of the in-plane strain induced by the disparate binding energies of the binaries, CdTe and ZnTe in the CdZnTe lattice and certain miscibility issues. To solve this problem, the Army Research Laboratory research staff has developed a new substrate technology that utilizes selenium instead of zinc to produce CdSeTe/Si, which can be lattice matched to HgCdTe through control of the Se composition. CdSeTe offers optimum lattice matching capability without the complications of in-plane strain and miscibility issues.

In this paper we describe some of our technical findings related to this new discovery and discuss further results using quaternary CdZnSeTe/Si as a solution for both, mid-wave and long-wave large-format high-resolution IRFPA development. In this work, CdSeTe/Si, and CdZnSeTe/Si have been grown and studied using molecular beam epitaxy (MBE). When the concentration of Zn and/or Se is carefully chosen, the composite substrate can obtain exact lattice matching to HgCdTe, which will minimize the dislocations generated at the epilayer-composite substrate interface, further advancing device performance. Of these ternary and quaternary alloys, each has unique crystalline characteristics as result of cation (Zn) mixing, anion (Se) mixing or balanced cation and anion mixing.

Through this effort to further advance composite substrate technology, the future of HgCdTe material utilization for advanced IR systems is wide-open. Additionally, Si-based composite substrate have potential uses in other advanced semiconductor device systems, such as development of improved material for thermo-electric (TE) cooling as well as thermal photovoltaic (TPV) power generation.

2. EXPERIMENTAL PROCEDURES

All Cd-based II-VI materials for this study were grown on Si(211) nominal substrates in a three-inch molecular beam epitaxy (MBE) system from DCA instruments (Turku, Finland). The MBE system was equipped with binary CdTe and ZnTe effusion sources along with elemental Se, Cd, and As sources. Standard Si substrate cleaning processes were utilized for this study. Further details of the layer structure and growth processes have been described elsewhere (Chen et al, 2003, Chen et al, 2004). $CdSe_xTe_{1-x}$ was grown with $0 \le x \le 1$ to study the fundamental bandgap and material properties as a function of Se content. $Cd_{1-y}Zn_ySe_xTe_{1-x}$ layers were grown with x + y kept near 0.04 in order to study the role of Zn and Se incorporation on material properties while maintaining lattice matching with HgCdTe. Additionally, optical measurements were conducted on a set of these quarternary layers. Finally, both CdTe and CdSe layers were grown to establish baseline parameters and properties.

Structural characterization was conducted using both X-ray diffraction and transmission electron microscopy (TEM). The full width at half maximum (FWHM) taken from double crystal rocking curve (DCRC) measurements of the {422} diffraction peaks from the Cd-based II-VI layers were measured to assess the general crystalline quality of the material. Additionally, x-ray diffraction was used to determine the overall composition of the ternary and quarternary layers with respect to CdTe while wavelength dispersive x-ray analysis (WDX) was used to determine the individual concentrations of Zn and Se incorporated within quarternary layers (Chen et al, 2004). The material's crystal structure was examined using transmission electron microscopy (TEM) diffraction patterns obtained with a JEOL 2010F TEM operated at 200 keV. Finally, optical microscopy was used to observe surface morphology and defect density as a function of layer composition.

Optical measurements were also carried out using room temperature photoluminescence (PL) and photoreflectance (PR) to measure the response in the near bandgap (E_g) region. Measurements were taken on both $CdSe_xTe_{1-x}$ with x ranging from 0 to unity and on $Cd_{1-y}Zn_ySe_xTe_{1-x}$ with x + y = 0.04 but with x and y individually varying between 0 and 0.04. PR spectra were acquired using a Semiconductor Characterization Instruments' automated photoreflectance system* (Pollack, 1994). Spectra were recorded over the near bandgap region extending from 1 eV to ~1.9 eV with a spectral resolution of 1 meV. The pump source was a 442

* Certain commercial products are identified in the manuscript to adequately specify the procedure. This does not imply recommendation or an endorsement, nor does it imply that they are the best available for the purpose.

nm line derived from a He-Cd laser with an average power density of the pump source at the sample surface of ~5 mW/cm^2. The detector was a thermoelectrically cooled InGaAs photodiode. PL measurements were performed at room temperature using a conventional system comprised of a laser excitation (Kr^+, 647.1 nm line), a monochromator, and a Si detector.

3. RESULTS AND DISCUSSION

3.1 CdSeTe/Si Properties

Incorporation of Se into the CdTe matrix was investigated by growing $CdSe_xTe_{1-x}$ throughout the entire composition range ($0 \leq x \leq 1$). Optimal MBE growth conditions were established for low Se ($x < 0.05$) CdSeTe material growth with subsequent characterization suggesting very high quality material had been obtained (Chen et al, 2003). X-ray diffraction FWHM data from the CdSeTe layers (~ 5 μm thick) on average measured 125 arcsec with a low value of 97 arcsec obtained. Additionally, layers exhibited a smooth surface morphology with a low level of surface defects, typically less than 500 cm^{-2}. It should be noted that all CdSeTe layers nucleated with $x \leq 0.05$ grew in the cubic crystal phase as determined by the presence of the {422} x-ray diffraction peak. Using these same growth conditions, $CdSe_xTe_{1-x}$ layers were grown with x increasing to unity. Since the CdTe binary compound is a zincblende crystal while the CdSe binary compound is a wurtzite crystal, it is reasonable to expect a phase change in crystal structure at some Se composition within the $CdSe_xTe_{1-x}$ material system as we go from CdTe ($x = 0$) to CdSe ($x = 1$). This has been reported for $CdSe_xTe_{1-x}$ grown on glass substrates with zincblende material nucleated for $x < 0.60$ and wurtzite material nucleated for $x > 0.60$ (Sebastian et al, 1991). Similarly, Bridgman grown bulk $CdSe_xTe_{1-x}$ was found to nucleate as zincblende for $x \leq 0.45$ and as wurtzite for $x \geq 0.65$ with a mixed phase for $0.45 \leq x \leq 0.65$ (Schenk et al, 1998).

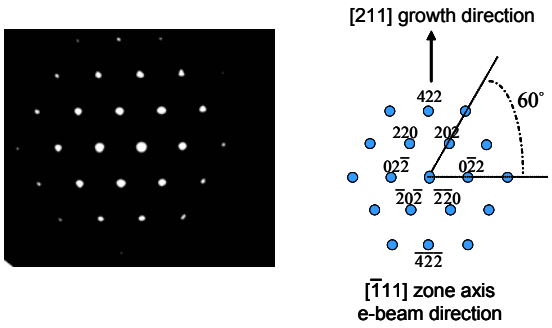

Fig. 1. TEM diffraction pattern indicating cubic CdSe had been grown. Similar results were obtained for all CdSeTe layers grown for this study.

However, our observation of the {422} x-ray diffraction peak clearly indicated that $CdSe_xTe_{1-x}$ remained in the cubic phase throughout the entire composition range for the MBE growth conditions used in this study. CdSe has been reported to grow in the cubic phase on GaAs (Samarth et al, 1989; Matsumura et al, 2000) and ZnSe substrates (de Melo et al, 2003), but this is the first reported observation of cubic $CdSe_xTe_{1-x}$ material grown throughout the entire composition range. Furthermore, we were able to nucleate cubic material on Si substrates. Electron diffraction patterns along orthogonal zone axes [1 -1 0] and [-1 1 1] were also taken with the TEM system to further confirm that high Se content CdSeTe layers were cubic. Figure 1 shows the TEM diffraction pattern from a CdSe layer grown on a Si substrate. Included in the figure is the expected diffraction pattern from a cubic crystal. Similar TEM diffraction patterns were observed for $CdSe_xTe_{1-x}$ with $x = 0.75$ and $x = 0.91$ confirming zincblende material growth throughout the entire composition range.

Room temperature PL and PR measurements were also made on these layers to determine the bandgap as a function of Se concentration. Figure 2 shows typical PL and PR data taken at room temperature.

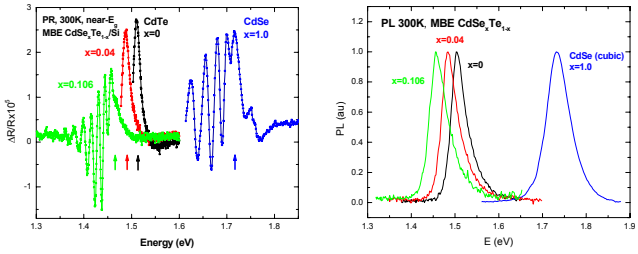

Fig. 2. Photoreflectance (PR) and photoluminesence (PL) data from CdSeTe layers.

Intense luminescence and photoreflectance data with good signal to noise ratio were readily obtained from the CdSeTe layers with identification of the bandgap made simply from the position of the main spectral feature. A clear shift in the bandgap with respect to CdTe is observed dependent on the alloy composition.

Figure 3 shows the bandgap dependence on x for low Se incorporation ($x \leq 0.15$), the composition range of technological interest for lattice matching to HgCdTe. This data shows a linear relationship between Se composition and bandgap, for low x values. This data will be useful in obtaining full wafer uniformity maps of the Se composition over large areas both quickly and in a non-destructive manner, which is vital at both a scientific and production level. To date, there is a significant lack of data on the CdSeTe material system within the open literature making this type of study even more significant.

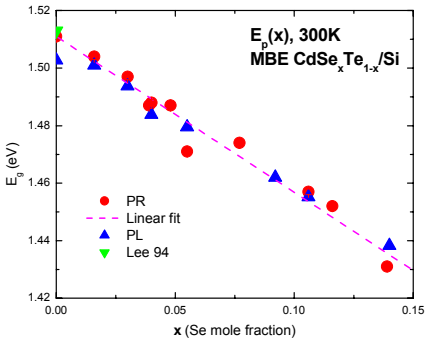

Fig. 3. $CdSe_xTe_{1-x}$/Si bandgap as a function of Se composition ($x \leq 0.15$) as determined by room temperature PL and PR measurements.

From the data, an equation for bandgap, E_g, as a function of Se composition, x, is obtained:

$$E_g(eV) = (1.511 \pm 0.001) - (0.539 \pm 0.004)x \qquad (1)$$

In addition to the work conducted on low x-value CdSeTe material designed to lattice match with HgCdTe, several layers were grown with higher x-values in order to study the entire composition range. Figure 4 shows the bandgap data as a function of alloy composition over the entire CdSeTe/Si composition range.

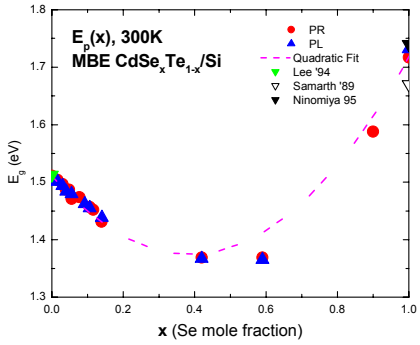

Fig. 4. $CdSe_xTe_{1-x}$/Si bandgap as a function of Se composition ($0 \leq x \leq 1$) as determined by room temperature PL and PR measurements.

From the data, a large bowing factor is observed for CdSeTe material. Using a quadratic fit of the data while holding the endpoints fixed, the bowing factor, $b_g(eV) = 0.996 \pm 0.004$ is obtained. This value fits with reported results of the CdSeTe bowing factor of 0.90 (Poon et al, 1995) and 0.94 (Prytkina, 1968) which were determined from $Cd_{1-x}Se_xTe$ layers with $x \leq 0.5$. The large bowing factor has been attributed to non-random ordering of the CdSeTe crystal. Poon et. al. have shown that a AuCu-I-like structure with 67% relaxation of the alloy will account for the large bowing factor found in CdSeTe material. Our results further support this conclusion based on our experimentally determined value of the CdSeTe bowing parameter derived from layers spanning the entire composition range.

3.2 CdZnSeTe/Si Properties

To study the role of anion mixing versus cation mixing within the CdTe matrix, $Cd_{1-y}Zn_ySe_xTe_{1-x}$ layers were nucleated and grown on Si substrates. The total goal composition (x + y) was kept constant near 0.04 while the constituent Zn and Se elements were varied individually approximately between 0 and 0.04 in order to maintain the overall lattice-matching properties of the layers to HgCdTe. X-ray diffraction measurements were made on the set of $Cd_{1-y}Zn_ySe_xTe_{1-x}$ layers, including ternary CdSeTe (y = 0) and ternary CdZnTe (x = 0). Results indicated no significant degradation of the crystalline quality with the incorporation of both Zn and Se, regardless of the individual constituent percentages.

However, the surface morphology of CdZnSeTe material shows a clear dependence on the level of Zn and/or Se incorporated into the layer. Figure 5 shows several optical microscopy images taken from CdZnSeTe layers as a function of both Zn and Se. As seen in the figure, the CdZnTe surface exhibits roughness even though the layer was grown near the optimal CdTe MBE conditions and had excellent x-ray FWHM data. However, as the Zn content is decreased and the Se content is subsequently increased, the surface roughness decreases substantially. For ternary CdSeTe, the surface is completely smooth and mimics that of the CdTe as-grown surface. All of these layers were grown under identical nucleation conditions.

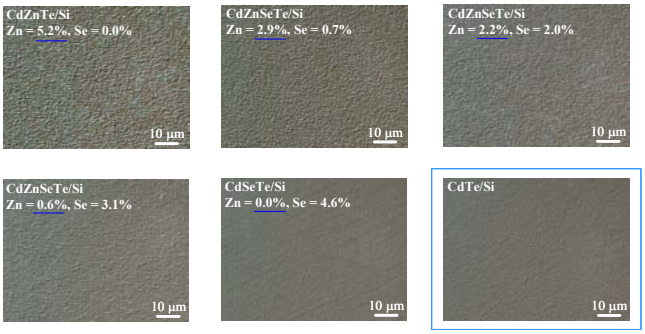

Fig. 5. Optical microscopy images of quarternary CdZnSeTe layers grown on Si substrates as a function of Zn (Se) content. The framed image shows a typical CdTe surface which is used as a benchmark.

These results further highlight ARL's motivation for developing a new composite substrate for HgCdTe material growth. Although adding Zn to the CdTe matrix will also achieve the desired lattice constant to achieve lattice-matching, the addition of Zn is not a trivial process.

The dislocation density of the CdZnSeTe material was also determined through use of the Everson etch

which is known to reveal dislocations within CdTe and CdZnTe (211) orientated material (Everson et al, 1995). Results indicate that when either "Zn-rich" (Se < 0.01 and Zn > 0.03) or "Se-rich" (Zn < 0.01 and Se > 0.03) $Cd_{1-y}Zn_ySe_xTe_{1-x}$ material was studied, the dislocation density was significantly lower than "evenly mixed" (Se ~ 0.02 and Zn ~ 0.02) $Cd_{1-y}Zn_ySe_xTe_{1-x}$ material, with an average value near 2 x 10^5 cm^{-2} versus an average value near 1.5 x 10^6 cm^{-2} respectively. This data indicates that evenly mixed quarternary material has an order of magnitude higher dislocation density than either CdSeTe or CdZnTe and would not be appropriate as a composite substrate. However, low Se or conversely low Zn quarternary material should be suitable for composite substrate utilization based on the dislocation density measurements. It should also be noted that CdSeTe layers grown in this study had a lower dislocation density value than similarly grown CdZnTe layers.

Further characterization was carried out with room temperature PL and PR to study the near bandgap region of the quarternary layers. Figure 6 shows typical PL and PR data respectively from CdZnSeTe layers. From the optical data, the bandgap energy is observed to shift dependent on the individual amount of Zn and Se incorporated even though the total composition (x + y) for these layers was kept near 0.04. Note that the PL spectra are organized in pairs to highlight this effect. When more Se is incorporated within the quarternary system with respect to Zn, the band-gap shifts to lower energies. In contrast, for "Zn-rich" material the band-gap shifts to higher energies.

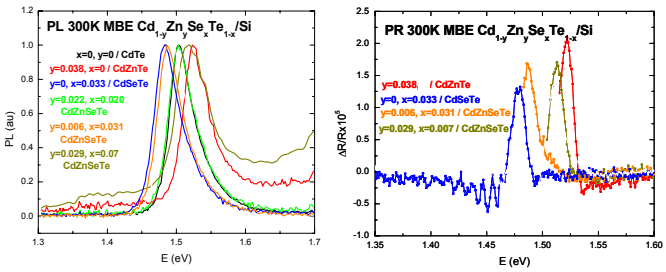

Fig. 6. PL and PR data from quarternary CdZnSeTe layers grown on Si substrates by MBE.

From the literature (Poon et al, 1995), the $Cd_{1-y}Zn_yTe$ bandgap energy shift for low y can be written as follows, if the quadratic term is dropped:

$$E_g(y) = 1.511 + 0.6y \quad \text{for } y \leq 0.10 \qquad (2)$$

Using this equation and equation (1), we can obtain the following expression for the bandgap shift for quarternary $Cd_{1-y}Zn_ySe_xTe_{1-x}$ layers. In units of eV, the resulting equation is:

$$E_g(x,y) = 1.511 - 0.54x + 0.6y \quad \text{for } x, y \leq 0.10 \qquad (3)$$

From this result, it is seen that Zn (y-value) and Se (x-value) shift the bandgap energy from the binary CdTe position nearly equal amounts but in opposite directions. This has been experimentally observed in our PL data (figure 6) which shows the peak from the quarternary layer with 2.2% Zn and 2.0% Se incorporated falling directly on top of the peak from the CdTe reference layer. This information further distinguishes the different growth mechanisms of cation (Zn) and anion (Se) mixed Cd-based II-VI material as was earlier demonstrated through the variation in surface roughness as a function of Zn and/or Se content (figure 5). This also indicates that the lattice constant and bandgap can be controlled independently for quarternary CdZnSeTe material. This fact might prove useful if advanced architectures, such as strained layer superlattices, are desired.

Figure 7 shows room temperature PR spectra from two quarternary layers. The PR spectra are similar to those seen from high-quality bulk samples with a distinct two-lobe feature in the vicinity of the bandgap, followed by a large number of oscillatory features at lower energies. A spectrum from a CdTe epilayer is also included for comparison.

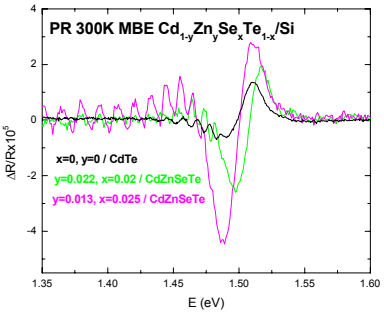

Fig. 7. Room temperature photoreflectance (PR) spectra from quarternary CdZnSeTe layers on Si substrates.

For these spectra, we used the well known Aspnes' three-point fit method to establish the bandgap values (Aspnes, 1980). We believe the near-E_g line-shape is due to a significant contribution from the excitonic component which is an indication of the high crystalline quality. The lower energy oscillations are due to interference fringes caused as a result of the large mismatch between the optical indices of the Si substrate and the epitaxial films. The presence of these fringes also attests to a uniform film with smooth and parallel interfaces, again an indication of high-quality films.

CONCLUSIONS

We have demonstrated high quality ternary and quarternary Cd-based II-VI growth utilizing MBE on Si

substrates. High quality CdSeTe/Si composite substrates have been grown and studied in order to achieve exact lattice matching to HgCdTe. $CdSe_xTe_{1-x}$ has also been demonstrated for the first time to remain in the cubic crystal phase throughout the entire range of Se compositions ($0 \leq x \leq 1$). Additionally, PL and PR optical experiments were conducted to study the optical response in the near bandgap region. Results indicated a large bowing of the bandgap as a function of composition which suggests a non-random ordering of the crystal. Quarternary CdZnSeTe material properties were also observed to be dependent on both Se and Zn content. Surface smoothness increased as the Se incorporation increased and the Zn incorporation decreased. The dislocation density of the material was observed to reach minimum values for either the case of low Se/high Zn content or low Zn/high Se content. Additionally, optical measurements made on these layers indicated that respective Zn and Se incorporation shift the quarternary bandgap away from the CdTe bandgap nearly equal amounts but in opposite directions.

Through this research effort, CdSeTe/Si composite substrates have been fabricated and studied with the goal of advancing subsequent HgCdTe material quality. This work will prove critical in the advancement of HgCdTe detector technology toward very high resolution systems fabricated at a reduced cost, elements which are key for Third Generation systems.

REFERENCES

D.E. Aspnes, Modulation Spectroscopy/Electric Field effects on the Dielectric Function of Semiconductors, in Handbook on Semiconductors Optical Properties of Solids, ed., M. Balkanski (North Holland, Amsterdam, 1980), Vol. 2., p.109.

Y.P. Chen, G. Brill, E.M. Campo, T. Hierl, J.C.M. Hwang, N.K. Dhar, 2004: *J. Electron Mater.,*. **33**, 6, 498.

Y.P. Chen, G. Brill, N.K. Dhar, 2003: *J. Crys.Growth*, **252,** 270.

Y.P. Chen, G. Brill, N.K. Dhar, 2003: *J. Elec. Mater.,* **32**, 7, 723.

O. de Melo, C. Vargas-Hernandez, I. Hernandez Calderon, 2003: *Appl. Phys. Lett.,* **82**, 1, 43.

N.K. Dhar, C.E.C. Wood, A. Gray, H.Y. Wei, L. Salamanca-Riba, and J.H. Dinan, 1996: *J. Vac. Sci. Technol. B*. **14**, 2366.

W.J. Everson, C.K. Ard, J.L. Sepich, B.E. Dean, and G.T. Neugebauer, 1995: *J. Electr. Mater.,* **24**, 505.

N. Matsumura, J. Ueda, J. Saraie, 2000: *Jpn. J. Appl. Phys.* **39**, L1026.

F.H. Pollak, Modulation Spectroscopy of Semiconductors and Semiconductor Microstructures, in Handbook on Semiconductors: Optical Properties of Semiconductors, edited by M. Balkanski (North Holland, Amsterdam, 1994), Vol. 2, p. 527.

H.C. Poon, Z.C. Feng, Y.P. Feng, and M.F. Li, 1995: *J. Phys. Condens. Matter.,* **7**, 2783.

L.V. Prytkina, V.V. Volkow, A.N. Vanyukow, and P.S. Kireev, 1968: *Sov. Phys.-Semicond.* **2,** 509.

S. Rujirawat, L.A. Almeida, Y.P. Chen, S. Sivananthan, and D.J. Smith, 1997: *Appl. Phys. Lett.,* **71**, 1810.

N. Samarth, H. Luo, J.K. Furdyna, S.B. Qadri, Y.R. Lee, A.K. Ramdas, N. Otsuka, 1989: *Appl. Phys. Lett.,* **54**, 26, 2680.

M. Schenk, C. Silber, 1998: *J. of Matls Sci*.: Materials in Electronics, **9**, 4, 295.

P.J. Sebastian, V. Sivaramakrishnan, 1991: *J. Crys. Growth,* **112**, 421.

P.S. Wijewarnasuriya, M. Zandian, D.D. Edwall, W.V. McLevige, C.A. Chen, J.G. Pasko, G. Hildebrandt, A.C. Chen, J.M. Arias, A.I. D'Souza, S. Rujirawat and S. Sivananthan, 1998: *J. of Electronic Mater.*, **27**, 546.